Highly Underactuated Radial Gripper for Automated Planar Grasping and Part Fixturing

Vatsal V. Patel, *Student Member*, IEEE, Andrew S. Morgan, *Student Member*, IEEE, and Aaron M. Dollar, *Senior Member*, IEEE

***Abstract*—Grasping can be conceptualized as the ability of an end-effector to temporarily attach or fixture an object to a manipulator—constraining all motion of the workpiece with respect to the end-effector's base frame. This seemingly simplistic action often requires excessive sensing, computation, or control to achieve with multi-fingered hands, which can be mitigated with underactuated mechanisms. In this work, we present the analysis of radial graspers for automated part fixturing and grasping in the plane with a design implementation of a single-actuator, 8-finger gripper. By leveraging a passively adaptable mechanism that is under-constrained pre-contact, the gripper conforms to arbitrary object geometries and locks post-contact as to provide form closure around the object. We also justify that 8 radially symmetric fingers with passive locking are sufficient to create robust form closure grasps on arbitrary planar objects. The underlying mechanism of the gripper is described in detail, with analysis of its highly underactuated nature, and the resulting form closure ability. We show with a wide variety of objects that the gripper is able to acquire robust grasps on all of them, and maintain maximal quality form closure on most objects, with each finger exerting equal grasp force within ±2.48 N.**

***Index terms*—Mechanical Design, Mechanism, Fixturing, Manufacturing, Form Closure, Grasping**

I. Introduction

An object is considered to be fixtured to a base frame if all motions of the workpiece are fully constrained given the current state of the contacts. This implies that the fixtured object is able to resist any external wrenches or perturbations applied, fundamentally attaching the object to a rigid body. Equivalently, robot grasping can be regarded as the ability to temporarily attach an object to the end of a robot manipulator, constraining all motion with respect to the gripper frame. This allows the manipulator to reposition or reorient the object efficiently, without considering additional dynamics associated with the workpiece. Many traditional approaches to grasping and part fixturing require object-specific computation and modeling to define the location of the contacts. By leveraging a passively adaptable mechanism that is able to conform to the contours of arbitrary objects, a potential solution to automated part fixturing and grasping is introduced for use in both manufacturing and robotic applications.

Fixture design in manufacturing relies on widely used heuristics such as 3-2-1, which requires that the part to be fixtured contacts the primary datum feature at 3 points, the secondary datum feature at 2 points, and the tertiary datum feature at 1 point [1]. Most automated processes still use single-purpose jigs designed and fabricated for particular parts, which can be very time consuming and expensive to manufacture. Thus, easily adaptable manufacturing systems are limited by the flexibility of the fixturing solutions [2]. Modular fixturing systems aim to automate the fixture design process by incorporating prior knowledge of the object's shape and orientation. These systems include design algorithms using the peg/hole devices in 2-D with a single degree of freedom [3], [4], and were touted as universal grippers when inverted or mounted on a robot arm. This implementation was then later extended to a 3-D design tool [5]. However, these approaches required specialized translating fixture tables, and still necessitated manual setup of peg placement, although guided by the algorithm's output. More importantly, the algorithms rely on accurate information known *a priori* of the object's silhouette and pose to determine fixture point locations, which may not always be available.

Fig. 1. The proposed 8-finger single-actuator fixturing gripper mounted on a robot arm and grasping planar lamina. Each finger translates radially inward until it comes in contact and exerts the same force on the lamina. Upon contact, the fingers lock passively and create a form closure grasp.

Robotic grasping is equivalent to fixturing in its goal – restraining objects using a suitable set of contact constraints [6]. In robotics literature, these constraints applicable to robotic grasping are typically referenced under two different classifications: *form closure* and *force closure.* In the former, a set of contacts are said to exhibit *form closure* if all motions of the object can be prevented given an external wrench (force and torque) with frictionless point contacts [7]. Because the points are frictionless, it has been shown that this property is purely geometric [8]. Alternately, a set of frictional contact points are said to exhibit *force closure* if the contact wrenches applied to the object are able to equilibrate to any external wrench [9]. Formally, there exists a duality between these two fixturing classifications, where force closure has the same mathematical model as form closure if the contacts are

This work was supported by the United States National Science Foundation under Grant IIS-1734190.

V. V. Patel, A. S. Morgan, and A. M. Dollar are with the Department of Mechanical Engineering and Materials Science, Yale University, USA ({V.Patel, Andrew.Morgan, Aaron.Dollar}@yale.edu).

frictionless [10], [11]. Moreover, the form closure property has also been studied in the context of underactuated hands, wherein additional non-backdrivable mechanisms are required to affix the contacts in space [12]–[14].

In this work, we present a novel single-actuator, 8-finger fixturing device that is able to provide planar form closure by inherently conforming to arbitrary object shapes and passively locking the contact points (Figure 1). The grasper leverages a tendon-based differential that provides equal force to all 8 fingers. As the fingers are actuated, compression springs counteract the actuation as to supply a return force. The fingers are arranged on prismatic joints in a circular pattern equidistant from one another. Each finger is individually equipped with a passive locking mechanism, which constrains translation motion of a single finger after object contact in order to provide form closure. The remaining fingers are free to translate until contact is made and all fingers are eventually locked.

Few previous works have attempted to develop a mechanical solution to automated part fixturing [15]. Single-actuator radially-symmetric prismatic grippers have been implemented in robot grasping previously [16], and highly underactuated mechanisms have also been adopted for underwater grasping [17]. To the best of the authors' knowledge, this is one of the first works to develop a highly underactuated grasper with passive locking for application in planar grasping and part fixturing. The continuation of this paper is organized as follows: Section II analyzes the form closure capability of multi-finger radial grippers, Section III describes the design of the 8-finger implementation, Section IV presents an experimental validation of the design and characterization of the force distribution across the fingers, and finally, Section V summarizes the results and discusses improvements that can be made to the gripper in the future.

II. Form Closure Analysis

The location and number of contacts play an important role in ensuring form closure for any grasp. For the radially symmetric configuration, first we need to evaluate the number of fingers required to robustly grasp arbitrary objects with form closure. In 1876, Reuleaux studied rigid lamina in the plane and showed that at least four point contacts (or contact wrenches) were required to resist all motion of the lamina given an external wrench [18]. Later, this work was extended to show that at least seven higher-order (point) contacts were required to fully constrain an object in 3D space [19]. Several works in the robot grasping and manipulation community have since attempted to generalize the number of contacts required to constrain object motion for both, form closure and force closure [20]. In addition to the works aforementioned, that in [8] generalized the conditions for form closure, noting that at least *m+1* contacts are required to fully constrain object movement in an *m-dimensional* subspace. An upper bound on the number of frictionless point contacts required was also found in [21] for arbitrary objects. That is, in the planar case, **4** contact points would be necessary and sufficient for constraining object movement. For form closure, [22] proved that three/four contacts with friction were sufficient to constrain an object in 2D/3D for force closure, respectively. This promoted further investigation given specific contact models, which was formulated in [23] for both hard and soft contacts.

We require our gripper to create form closure grasps and thus model the contacts as frictionless points. This is a stricter design constraint than modeling contact points with friction or requiring just force closure considering applications of the gripper in part fixturing, wherein objects would need to be fully immobilized.

To evaluate the number of radial, equidistant fingers required on a gripper such that a form closure grasp can be found for any 2D object, we simulated contact points created by $N = 4, 5, 6 \ldots 12$ radially symmetric fingers on 100 randomly generated 2D object silhouettes. The point contacts were identified at the intersection of the object silhouette and N radially symmetric rays originating from the centroid of the silhouettes. The resulting contact points on each of the objects for an N-fingers case were then tested for form closure using the quantitative test outlined in [7]. Since 4 points out of N are necessary and sufficient to create form closure, all combinations of 4 contacts from the N contact points were tested for form closure for the combination with the highest quality metric from [7] described below.

The form closure property for a configuration of contact points can be checked by looking at the null space vectors $\boldsymbol{d_{n,null}}$ of the normal wrench matrix $\boldsymbol{W_n}$. Only the normal component of the contact wrench matrix is considered since the contacts are assumed to be frictionless points, and cannot apply any force tangential to the object surface. For the planar case, $\boldsymbol{W_n}$ is $3 \times n_c$, where n_c is the number of contacts, and is formed by horizontally concatenating the 3×1 normal wrench $\boldsymbol{W_{n,i}}$ vector for each contact. These vectors can be calculated using the unit inward normal $\boldsymbol{\hat{n}_i}$ at each contact point location $\boldsymbol{p_i}$:

$$\boldsymbol{W_{n,i}} = \begin{bmatrix} \boldsymbol{\hat{n}_i} \\ \boldsymbol{p_i} \times \boldsymbol{\hat{n}_i} \end{bmatrix} \in \mathbb{R}^{3\times 1} \tag{1}$$

$$\boldsymbol{W_n} = [\boldsymbol{W_{n,1}} \quad \boldsymbol{W_{n,2}} \quad \ldots \quad \boldsymbol{W_{n,n_c}}] \tag{2}$$

We can now calculate the null space vectors $\boldsymbol{d_{n,null}}$ of the normal wrench matrix $\boldsymbol{W_n}$ and check if any of these vectors are positive.

$$\boldsymbol{W_n d_{n,null}} = \boldsymbol{0} \tag{3}$$

$$\text{Check: } \boldsymbol{d_{n,null}} > \boldsymbol{0} \tag{4}$$

If there exists any such $\boldsymbol{d_{n,null}} > \boldsymbol{0}$, then the contact points are said to create form closure. Otherwise, no form closure grasp exists for the particular set of contact locations on the given object. The metric Q_{FC} used to indicate the quality of the form closure, i.e. how far the contact points are from losing their form closure property, is calculated by looking at the minimum element $d_{n,null_k}$ in each $\boldsymbol{d_{n,null}}$ vector. The largest of all the $d_{n,null_k}$ values is noted as the form closure quality metric Q_{FC} for the grasp. Note that for any value of $Q_{FC} > 0$, the grasp is form closure, and only for $Q_{FC} = 0$ the contact configuration around the object fails to satisfy this property. Also, since normalized null space vectors are used, the size of the object silhouettes does not matter, and values of Q_{FC} for a contact configuration can range from 0 to 1.

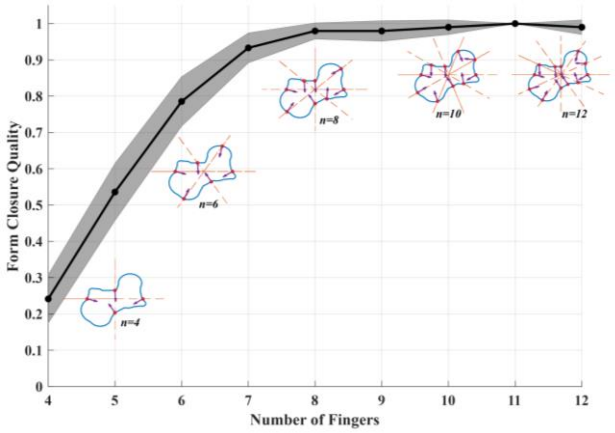

Fig. 2. Average form closure quality, Q_{FC}, for 100 randomly generated, non-convex object silhouettes while varying the number of radially symmetric fingers. Error region corresponds to ±2 standard deviations.

$$Q_{FC} = \max\left\{\min_{k}\left\{ d_{n,null_k}\right\}\right\} \text{ where, } \boldsymbol{d_{n,null} > 0} \quad (5)$$

Figure 2 shows the results of the average of form closure quality, Q_{FC}, across the 100 randomly generated object silhouettes for increasing number of the gripper fingers. An example random object silhouette is also shown for N = 4, 6, 8, 10, and 12 cases along with the inward normal at each identified contact point. In the 4- and 5-fingers cases, there is a significant number of objects where a form closure grasp cannot be found. And even for objects where a form closure grasp can be created, the quality, Q_{FC}, of grasp is not high. Thus, an external wrench might be able to free the object should there be any error in expected contact locations, or insufficient normal force at a contact point. In the 6- and 7-fingers cases, there are still some objects for which either a form closure grasp cannot be found or Q_{FC} is low. In order to create robust form closure grasp for almost all the objects, at least 8 or 9 fingers are required. All the tested objects were able to be grasped with form closure with more than 8 fingers, and the resulting grasps were robust to any limitations of a physical prototype as noted by their high corresponding Q_{FC} values. The design we implemented chose the 8-finger configuration in order to have pairs of fingers facing directly opposite to each other, which was necessary to minimize pre-grasp object motion described in Section III.A.

Note that even higher number of fingers also result in finding robust form closure grasps for all the objects. However, such configurations have a more limited workspace range in a physical implementation due to the size of the various components and interference caused by adjacent fingers running into each other during grasping.

III. Mechanism Design

The proposed fixturing gripper consists of 8 fingers which are mounted to sleeve bearing carriages on linear rails. The components are housed between two acrylic plates to create a flat, unobstructed palm for objects to be placed prior to fixturing or grasping (Figure 3 (a)). The rails are radially arranged such that they are equidistant from one another, and support prismatic actuation of the fingers to grasp and release objects in the plane. Finger bases are mounted on top of each of the carriages, and host the pulley for the input tendon and finger return compression spring (Figure 4). Molded fingers

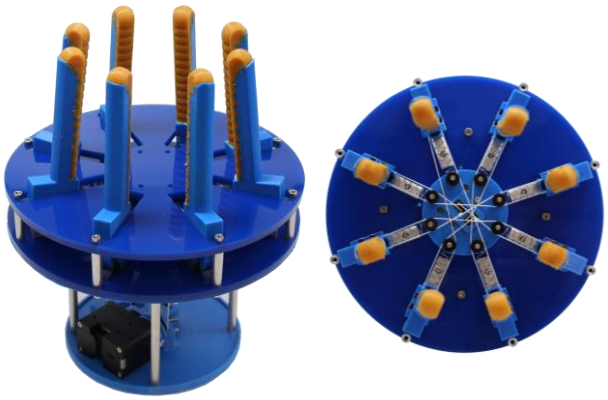

(a) **(b)**

Fig. 3. (a) Fully assembled single-actuator, 8-finger gripper. (b) Top view of the gripper with the palm plate removed. The tendon is routed between the fingers in the pattern shown for minimum wrapping angle around the fixed pulleys which leads to lower friction.

are then assembled on top of these finger bases through a pivot dowel, while a smaller compression spring for lock return is placed between the finger base and the molded finger. This spring serves to push the finger forward and keep the lower end of the finger clear of the linear rail when no contact has been made with an object (Figure 5). After contact, the moment due to contact force rotates the finger about the locking pivot joint, and the lower end of the finger creates friction against the linear rail to lock the finger in place. Rubber pads are glued to this end of the finger in order to accentuate the frictional force between the finger and the linear rail. This passive locking mechanism is key to creating form closure grasps which requires fixed contacts. Depending on the position of the contact along the finger, the locking mechanism activates with 1.5–2 N of force, which is well below the grasping forces observed in Section IV.B. Notably, if the object contact force increases, so does the frictional locking force because the moment due to the contact force pushes the rubber pads against the rail and increases the frictional force. Lastly, the direction of this friction force is same as that applied by the actuator tendon, and the locking mechanism does not interfere with the grasping action of the finger. That is, the locking force desirably scales with the object contact force while grasping force remains unaffected.

A single actuator (Dynamixel XM-430) is mounted on a 3D printed base under the bottom acrylic plate. The input force is transmitted to the 8 fingers through a tendon-driven differential (Section III.A). The applied motor torque was fixed at 2.46 Nm during testing, however output force at the fingers is proportional to the input motor torque which can go up to 4.1 Nm. The motor actuates the grasping motion of the fingers, and finger return springs pushing against the finger bases revert the fingers back to the open configuration after each grasp. Compression springs are used for the return actuation to retain the maximum amount of the prismatic finger travel range, while keeping a compact overall footprint of the gripper.

The fingers are 9 cm tall and designed with a 3D printed backing atop which a polyurethane ridged face is molded. The backing adds rigidity to the finger for higher force applications, while the polyurethane surface can conform to object corners and similar discontinuities, as well as apply

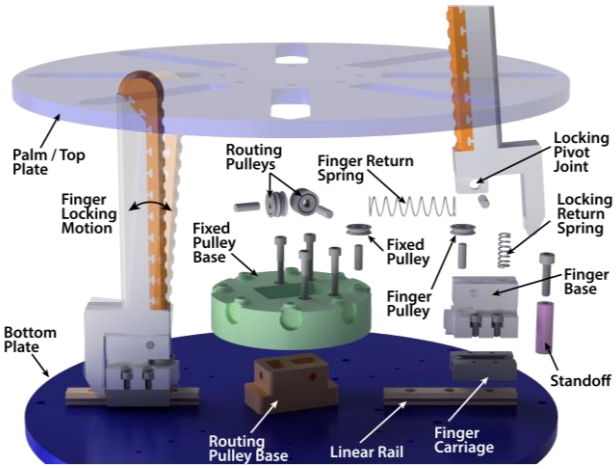

Fig. 4. Exploded view of one of the finger components and tendon routing bases. The locking mechanism is illustrated for the finger on the left – the contact force from the object engages the friction lock on the rail.

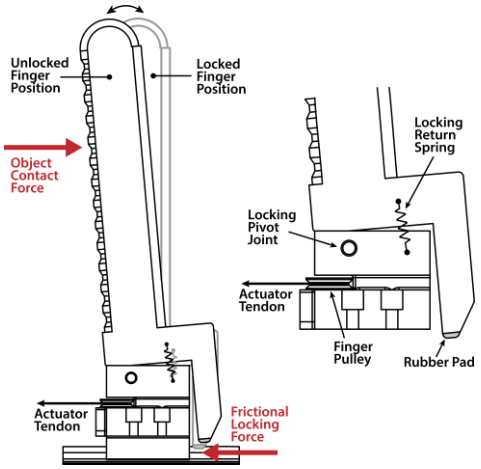

Fig. 5. The passive locking mechanism to enable form closure grasps actuates on contact with the object and generating friction in the grasping direction. The higher the contact force, the higher the resulting locking force.

frictional forces tangent to the object surfaces if needed. While the contact points are modeled as frictionless in Section II, surfaces of revolution such as cylindrical objects can only be grasped with friction contacts. Lastly, the small width of the fingers (11.5 mm) allows them to be pushed into tight spaces around non-convex objects, and prevents interference with adjacent fingers for small objects.

The workspace range of the gripper is determined by two main factors: the overall diameter of the gripper, and the offset between the finger and the carriage. Evidently, a large diameter gripper would allow space for longer linear rails, and thus, enable objects with a larger diameter to be grasped. On the other hand, the smallest object that can be grasped is determined by the offset between the fingers and the carriage. Because the carriage blocks are limited by their width when travelling radially inward, the fingers can be offset towards the center of the gripper if smaller radius objects are needed to be grasped. Note that this also affects the maximum diameter of the graspable objects. For our proof-of-concept gripper, the fingers are mounted with zero offset i.e. directly above the carriage blocks for simplicity, and 50 mm long linear rails are used with 17 mm wide carriage blocks. With these parameters, the overall diameter of the gripper is 200 mm, and subsequently, the smallest and largest radii of objects that can be grasped are 56 mm and 122 mm respectively. The fingers can be offset or different length linear rails can be used if the range is determined unsuitable for certain applications.

A. Tendon-driven Differential Design

A differential is required to drive 8 fingers with a single motor because equal force needs to be applied at each of the outputs, and fingers need to conform to various objects without *a priori* knowledge of pose or shape. The main challenge of implementing such a single actuator gripper with a large number of fingers is designing a differential that can split input equally across the many outputs. While pneumatic differentials have been used in grasping applications [24], the device complexity and size for a gripper increases with the number of outputs. For instance, an *N*-finger grasper would require *N* air cylinders to drive each of the finger outputs. Taking into account the physical limitations of differential options, a tendon-driven differential is implemented to actuate our gripper.

The 1-input to 8-outputs differential is carried out in 2 phases (Figure 6). The first phase employs 2 levels of floating pulleys to split the input from the motor into 4 outputs. In the second phase, these 4 outputs are then routed with a single tendon through 2 finger bases each, inspired by a differential similar to the one described in [25]. The single tendon ensures that output forces at each of the fingers are equal, and allow the fingers to translate individually even after some have made contact. Another major challenge of splitting to large number of outputs is that a large displacement is required at the input in order to drive all the outputs (because of the inverse force and displacement relationship for constant work). While anchoring the ends of the single tendon halves the required input displacement, a tall structure beneath the bottom acrylic plate is still required to allow all the differential components to displace without interference. The main drawback of such a multi-stage differential is that the friction at the various components can result in unequal force distribution at the different outputs, and this is evaluated for our gripper in Section IV.B.

In order to mitigate these issues to some extent, the tendon was routed such that the wrapping angle around the fixed pulleys was minimized (Figure 3 (b)). This has two advantages in improving synchronization of finger closing action and output forces at contact points. First, the fingers facing each other are adjacent in the tendon route; so, any differences in force drop-off due to friction in the tendon is minimal for pairs

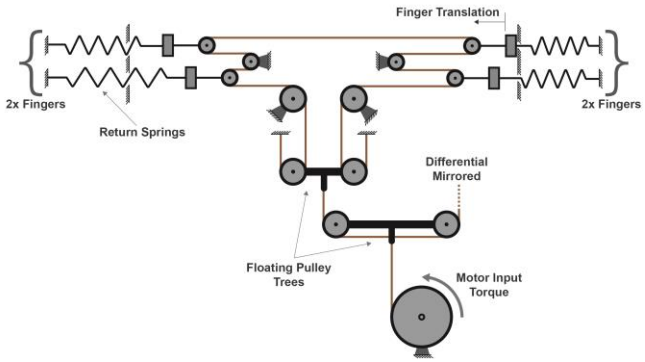

Fig. 6. The routing schematic for one half of the 1-input-4-output differential is shown here. The output of this differential is then routed in a continuous loop between the fingers that ensures equal force output at each finger.

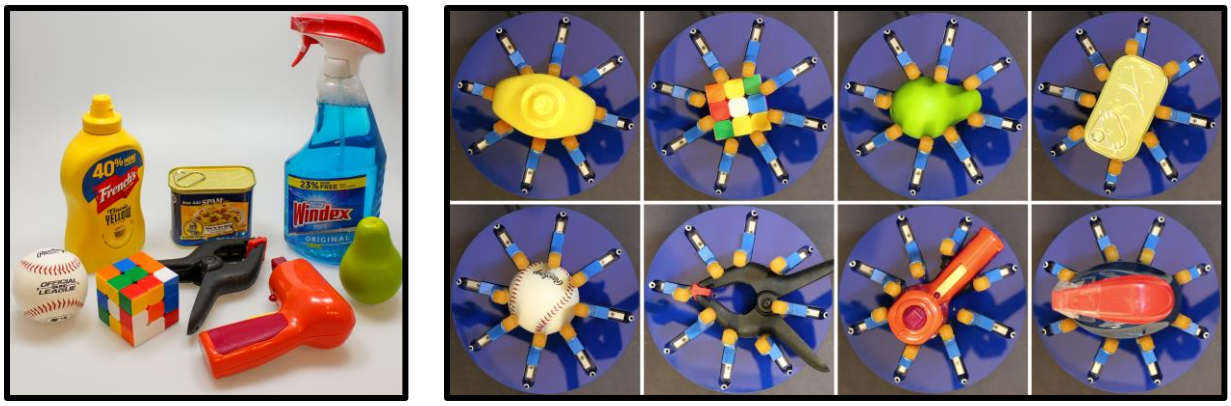

(a) **(b)**

Fig. 7. (a) YCB objects tested to validate efficacy of the proposed fixturing gripper design. The objects fit within the workspace of the gripper and provided a wide variety of profiles to test form closure in the plane. (b) Top view of the grasped objects shows the fingers contacting and locking around the objects.

of two opposite fingers. As a result, any two opposite fingers close radially in near-simultaneously and the output force at these fingers is equivalent. Second, the smaller wrap angle around the fixed pulleys in the middle results in a smaller net force applied to the pulleys, and thus, fewer frictional losses. This significantly improves the force transmission from the motor to the outputs.

IV. Experimental Results

We validated the efficacy of the proposed design by testing the form closure quality, Q_{FC}, on 8 objects from the YCB Object and Model Set [26]. The objects were selected to fit within the workspace range of the gripper, and for their wide variety of profiles in the plane. The gripper is systematically closed around each of object, and the object silhouette and contact points are extracted to calculate Q_{FC}. We then test the force exerted by each of the 8 fingers separately with a force gauge.

A. Form Closure Quality (Q_{FC}) on YCB Objects

We characterize the grasping capability of the gripper by grasping 8 objects selected from the YCB set, each with a different silhouette in the plane. This object test set includes the mustard bottle, Rubik's Cube, artificial pear, potted meat can, baseball, large clamp, toy power tool, and Windex bottle (Figure 7 (a)). Each object was placed approximately in the middle of the palm, and the Dynamixel torque was set to 2.46 Nm. The 8 objects fall within the workspace range, and each of them should be able to be grasped reliably. During the tests, minimal pre-grasp object motion was observed as all the fingers closed near-simultaneously. And for most of the objects, repeated grasps were independent of the initial location and pose of the objects. Each of the fingers' locking mechanisms were observed to engage when they made contact with the objects (Figure 7 (b)).

Some of the narrower objects such as the Rubik's Cube and the toy power tool resulted in fewer than 8 contacts on the object. However, the resulting grasp was still robust, and analyzed for form closure quality, Q_{FC}. For the toy power tool in particular, initial position of the object had some effect on the final grasp and number of contacts. The toy's initial position that caused least number of fingers to contact the object was sampled for this test to highlight a worst-case scenario. For larger objects such as the clamp, different initial poses of the clamp generated two different grasps. For instance, if one of the handles of the clamp was in between two fingers instead of one as shown, the contact points would be closer to the center of the object as fingers could sneak between the clamp handles. The grasp with only one finger between the two handles was sampled for this test as a worse-case. The quality, Q_{FC}, of the form closure grasp on each of the 8 objects is calculated by the process described below.

In order to evaluate the quality, Q_{FC}, of form closure for the grasps on the YCB objects, the shapes' silhouettes and the grasps' contact locations were extracted. This was carried out

Table 1. Grasped Objects Tested for Form Closure Quality by Extracting Shape Profile and Contact Points

Object	YCB ID	No. of Contacts	Form Closure Quality, Q_{FC}
Mustard Bottle	6	8	*1*
Rubik's Cube	77	7	*1*
Artificial Pear	16	8	*1*
Potted Meat Can	10	7	*1*
Baseball	55	8	*0**
Large Clamp	51	8	*1*
Toy Power Tool	72	6	*0.1008*
Windex Bottle	22	8	*1*

**Finite surfaces of revolution cannot be form closed* [10].

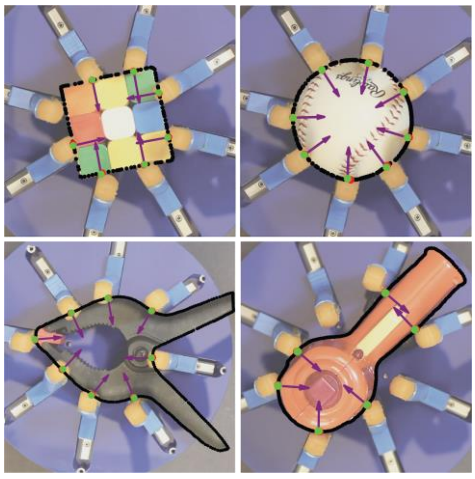

Fig. 8. Object silhouettes (black) and contact locations (green) are extracted from images, and the subsequent contact normals (purple) found on the nearest silhouette points (red) are tested for quality of form closure, Q_{FC}.

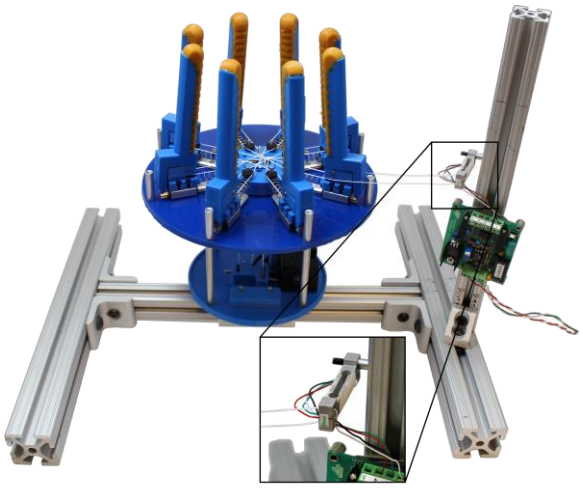

Fig. 9. Test setup for measuring force exerted by each finger. The gripper is rotated after each finger is tested in order to align the load cell with the translation direction of the finger. The process is repeated for each finger.

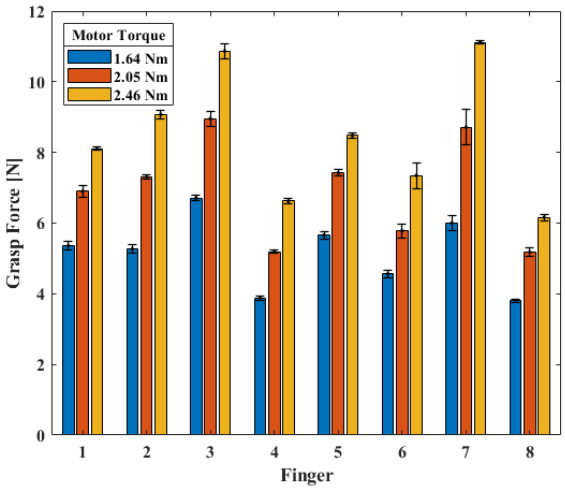

Fig. 10. Grasp force exerted by each of the 8 fingers for 3 different values of input motor torque. The variance in force across the fingers can be attributed to different friction magnitudes along the 4 differential outputs.

by manually tracing the contact points and silhouettes in the recorded images of the grasped objects, and running the same quality metric, Q_{FC}, calculation as described in Section II (Figure 8 illustrates this for 4 of the tested objects). The results of Q_{FC} for the 8 objects are detailed in Table 1. All of the objects except the baseball and the toy power tool are grasped with maximum Q_{FC} value. The Q_{FC} for the spherical baseball evaluates to 0 because the contacts are modeled as frictionless points, and thus a pure external torque applied about the center of the baseball cannot be resisted by these contacts alone. However, the high friction polyurethane padding on the fingers help create a robust force closure grasp for surfaces of revolution such as the baseball. For the toy power tool, Figure 8 shows that only 6 of the 8 fingers contact the object. And, the low Q_{FC} of the form closure grasp stems from the lack of any of those 6 contacts having normal force components at the base of the tool handle pointing towards the tool head. So, an applied external wrench in this direction could dislodge the object if some of the contacts were not able to provide sufficient normal force, or if the contacts moved under the external force.

B. Grasp Force Distribution across the Fingers

To validate the performance of the differential driving the 8 fingers, we devised a test setup to measure the grasp force exerted by each of the outputs (Figure 9). The setup consists of a straight bar load cell mounted on a frame and aligned with the line of actuation of the finger to be tested. A tendon is routed from the load cell to the finger pulley, so as to not actuate the locking mechanism. An amplifier circuit is added to log measurable voltage change from the load cell. The gripper is then commanded to close at 3 different values of input motor torque, and the force exerted by one finger is noted while the rest of the fingers close on an empty palm and hit hard stops. This test aims to highlight the losses due to friction, and consequent discrepancies in forces at the outputs of the differential. Figure 10 summarizes the results of testing the force applied by each finger for 3 input motor torques.

As expected, the output grasp force scales with the input torque. The grasp force at 2.46 Nm, which is the motor torque used in Section IV.A for the YCB objects, ranges between 6.16 N and 11.12 N across the fingers. More importantly, the grasp forces at opposite fingers (1-5, 2-6, 3-7, and 4-8) are nearly identical, indicating that the tendon routing prevents pre-grasp motion from unbalanced forces. There is a gradual drop in output force with any single tendon looping through outputs because the effects of friction add up away from the actuated ends. This is why the fingers immediately next to the floating pulleys (Fingers 1, 3, 5, and 7) can be expected to output higher grasp force than the remaining fingers (Fingers 2, 4, 6, and 8) that are somewhat weakened by friction from routing the tendon around a previous finger.

V. Discussion and Future Work

In this paper, we presented a novel grasping and fixturing gripper that utilized a single actuator and 8 radially arranged prismatic fingers to achieve form closure on arbitrary planar objects. The highly underactuated nature of the robot gripper allowed the fingers to conform to the objects easily, without any prior knowledge of the shape or orientation of the object. The tendon-driven differential and routing to minimize friction was suitable in implementing this single-input, multiple-output mechanism while retaining a compact gripper profile and sufficient workspace range. The passive locking mechanism allowed the fingers to be fixed in place after contact, which is a requirement for creating form closure grasps, and fundamentally differentiated this hand from other underactuated hands such as the SDM Hand [27] and the SoftHand [28]. We evaluated the ability of 8 fingers in simulation to find a form closure grasp and the quality of said grasp on arbitrary planar objects, and confirmed the results through physical experiments with YCB objects. The force distribution across the tendon differential was also recorded to characterize the effect of frictional drop-offs on the output forces.

Future work on the grasper will look into further reducing the effects of friction. One recommendation that has been proposed in [25] to reduce friction at the fixed pulleys is to combine them in a large pulley block with a separate cable going to the motor input. Although, the force output at the fingers is reduced by 1/*N*–times the motor input, and might require upgrading to higher torque actuator. Additionally, an extension of a similar mechanism might be effective in

fixturing and grasping in 3D space. Overall, the authors believe that underactuated mechanisms-based graspers and fixtures provide a faster, and more efficient method to create form closure grasps for applications in manufacturing and robotics, and thus warrant further exploration.

REFERENCES

[1] The American Society of Mechanical Engineers, *Mathematical Definition of Dimensioning and Tolerancing Principles, ASME Y14.5.1M - 1994*. New York: ASME, 1994.

[2] B. Shirinzadeh, "Issues in the design of the reconfigurable fixture modules for robotic assembly," *J. Manuf. Syst.*, 1993.

[3] A. S. Wallack and J. F. Canny, "Modular fixture design for generalized polyhedra," *Proc. - IEEE Int. Conf. Robot. Autom.*, vol. 1, no. April, pp. 830–837, 1996.

[4] R. C. Brost and K. Y. Goldberg, "A Complete Algorithm for Designing Planar Fixtures Using Modular Components," *IEEE Trans. Robot. Autom.*, vol. 12, no. 1, 1996.

[5] R. G. Brown and R. C. Brost, "A 3-D modular gripper design tool," *IEEE Trans. Robot. Autom.*, vol. 15, no. 1, pp. 174–186, 1999.

[6] C. Xiong, H. Ding, and Y. Xiong, *Fundamentals of Robotic Grasping and Fixturing*, vol. 3. WORLD SCIENTIFIC, 2007.

[7] J. C. Trinkle, "A Quantitative Test For Form Closure Grasps," in *Proceedings of the IEEE/RSJ International Conference on Intelligent Robots and Systems*, vol. 3, pp. 1670–1677.

[8] A. Bicchi, "On the Closure Properties of Robotic Grasping," *Int. J. Rob. Res.*, vol. 14, no. 4, pp. 319–334, Aug. 1995.

[9] H. Asada and M. Kitagawa, "Kinematic analysis and planning for form closure grasps by robotic hands," *Robot. Comput. Integr. Manuf.*, vol. 5, no. 4, pp. 293–299, Jan. 1989.

[10] V.-D. Nguyen, "Constructing force-closure grasps," in *Proceedings. 1986 IEEE International Conference on Robotics and Automation*, vol. 3, pp. 1368–1373.

[11] K. Lakshminarayana, *Mechanics of Form Closure*, PaperNo. 78-DET-32. New York: ASME, 1978.

[12] V. Bégoc, C. Durand, S. Krut, E. Dombre, and F. Pierrot, "On the form-closure capability of robotic underactuated hands," *9th Int. Conf. Control. Autom. Robot. Vision, 2006, ICARCV '06*, 2006.

[13] S. Krut, V. Bégoc, E. Dombre, and F. Pierrot, "Extension of the form-closure property to underactuated hands," *IEEE Trans. Robot.*, vol. 26, no. 5, pp. 853–866, 2010.

[14] S. Krut and V. Bégoc, "A simple design rule for 1st order form-closure of underactuated hands," *Mech. Sci.*, vol. 2, no. 1, pp. 1–8, 2011.

[15] H. Asada and A. By, "Kinematic analysis of workpart fixturing for flexible assembly with automatically reconfigurable fixtures," *IEEE J. Robot. Autom.*, vol. 1, no. 2, pp. 86–94, 1985.

[16] S. B. Backus and A. M. Dollar, "An Adaptive Three-Fingered Prismatic Gripper With Passive Rotational Joints," *IEEE Robot. Autom. Lett.*, vol. 1, no. 2, pp. 668–675, Jul. 2016.

[17] S. B. Backus, R. Onishi, A. Bocklund, A. Berg, E. D. Contreras, and A. Parness, "Design and testing of the JPL-Nautilus Gripper for deep-ocean geological sampling," *J. F. Robot.*, p. rob.21934, Feb. 2020.

[18] F. Reuleaux, *The Kinematics of Machinery*. London: Macmillan and company, 1876.

[19] P. Sommov, *Uber Gebiete von Schraubengeschwindig-keiten eines starren Korpers bie verschiedener Zahl vonStutzflachen*. Zeitschrift Mathematik Physik, 1900.

[20] B. Mishra, J. T. Schwartz, and M. Sharir, "Algorithmica On the Existence and Synthesis of Multifinger Positive Grips'," 1987.

[21] Y. Zheng and W.-H. Qian, "Coping with the Grasping Uncertainties in Force-closure Analysis," *Int. J. Rob. Res.*, vol. 24, no. 4, pp. 311–327, Apr. 2005.

[22] X. Markenscoff, L. Ni, and C. H. Papadimitriou, "The Geometry of Grasping."

[23] R. M. Murray, Z. Li, and S. Sastry, *A mathematical introduction to robotic manipulation*. CRC Press, 1994.

[24] V. Begoc, S. Krut, E. Dombre, C. Durand, and F. Pierrot, "Mechanical design of a new pneumatically driven underactuated hand," in *Proceedings 2007 IEEE International Conference on Robotics and Automation*, 2007, no. April, pp. 927–933.

[25] M. Baril, T. Laliberté, F. Guay, and C. Gosselin, "Static analysis of single-input/multiple-output tendon-driven underactuated mechanisms for robotic hands," *Proceedings of the ASME Design Engineering Technical Conference*, vol. 2, no. PARTS A AND B. pp. 155–164, 15-Aug-2010.

[26] B. Calli, A. Walsman, A. Singh, S. Srinivasa, P. Abbeel, and A. M. Dollar, "Benchmarking in Manipulation Research: Using the Yale-CMU-Berkeley Object and Model Set," *IEEE Robot. Autom. Mag.*, vol. 22, no. 3, pp. 36–52, 2015.

[27] A. M. Dollar and R. D. Howe, "The Highly Adaptive SDM Hand: Design and Performance Evaluation," *Int. J. Rob. Res.*, vol. 29, no. 5, pp. 585–597, Apr. 2010.

[28] C. Della Santina, C. Piazza, G. Grioli, M. G. Catalano, and A. Bicchi, "Toward Dexterous Manipulation With Augmented Adaptive Synergies: The Pisa/IIT SoftHand 2," *IEEE Trans. Robot.*, vol. 34, no. 5, pp. 1141–1156, Oct. 2018.